

Signal Enhancement in a Nonlinear Transfer Characteristic

M. E. Inchiosa* and A. R. Bulsara†

Space and Naval Warfare Systems Center, San Diego, Code D364, San Diego, California 92152-5001

A. D. Hibbs‡ and B. R. Whitecotton§

Quantum Magnetics, Inc., 7740 Kenamar Court, San Diego, California 92121-2425

(Received 2 July 1997)

We study nonlinear behavior in a model of a periodically modulated, overdamped rf SQUID loop operating in the dispersive (i.e., *nonhysteretic*) mode. In the presence of correlated noise we find an enhancement of the output signal-to-noise ratio (SNR) as a function of the nonlinearity parameter of the device. The calculation involves knowledge *only* of the input-output transfer characteristic of the device. These signal enhancement properties appear to be generic to devices characterized by nonlinear transfer characteristics. We also use our transfer characteristic approach to explain recent experimental results showing SNR enhancement in dc SQUIDs as a function of dc bias current and flux. [S0031-9007(97)05228-9]

PACS numbers: 05.40.+j, 02.50.Ey, 85.25.Dq

A series of publications in the past six years has explored the stochastic resonance (SR) phenomenon [1] in an rf SQUID loop [2] consisting of a superconducting loop interrupted by a Josephson junction. SQUIDs are the most sensitive detectors of magnetic fields, and SR offers a technique whereby their robustness to (external and sensor) noise could be substantially increased. All treatments to date, however, apply to the *hysteretic* mode of operation, corresponding to a multistable potential function.

In multistable SR devices, the lower the barrier between states, the higher the maximum output SNR. What if the barrier-producing nonlinearity is reduced up to and beyond the point at which the barrier disappears? Does the output SNR continue to increase with decreasing nonlinearity, or does it reach a maximum at a critical nonlinearity strength? To answer this question we consider the response of a *nonhysteretic* SQUID loop to a sinusoidal magnetic flux embedded in noise. We calculate the output SNR at the sinusoid's frequency via the SQUID transfer characteristic and find that *the SNR may be optimized as a function of β* , the nonlinearity parameter of the device.

In the nonhysteretic SQUID we do *not* find SR in the sense of SNR maximization as a function of input noise strength. This stems from our characterization of the SQUID as a *nondynamical* system characterized *only* by an input-output transfer characteristic; such a static characterization is predicated by the extremely small (see below) time constant of the device. A variant of SR in inertial, white-noise-driven, dynamical monostable systems with periodic signals, has been treated in the literature [3], and (for wideband signals) also demonstrated in models of single neurons and neural networks [4,5] with sigmoidal firing rate dependence, as well as in nondynamical systems without response thresholds [6] wherein the firing "rate" is assumed, *a priori*, to have a characteristic (Arrhenius-like) form. SR in nondynamical *threshold* detectors has also been the subject of many recent articles [1,7]. We

stress, however, that our archetypal system (the SQUID loop) does *not* have a level-crossing threshold, in contrast to the examples cited above; no transition or firing rate characterization of our system can be made.

In the rf SQUID [8], the magnetic flux $x(t)$ through the loop evolves according to the equation of motion $\tau_L \dot{x} = -U'(x) + x_e$. (We will measure all magnetic fluxes in dimensionless units of the flux quantum $\Phi_0 \equiv h/2e$.) The potential energy function $U(x) = \frac{1}{2}x^2 - \frac{\beta}{4\pi^2} \cos 2\pi x$ involves the nonlinearity parameter $\beta \equiv 2\pi LI_c / \Phi_0$, which is calculated from the loop inductance L and the junction critical current I_c . We apply an external magnetic flux $x_e(t) = x_i(t) + x_0$, where x_0 is a dc bias flux and $x_i(t) \equiv A \cos(\omega_0 t + \phi_0) + y(t)$ represents an input signal consisting of a sine wave (with a random initial phase) plus noise $y(t)$. The loop inductance and the normal state junction resistance R give rise to a very small time constant $\tau_L \equiv L/R$ of typically 10^{-10} to 10^{-12} sec, so that the SQUID bandwidth τ_L^{-1} far exceeds that of most signals of interest. The noise $y(t)$ may represent intrinsic or extrinsic noise, but in any case its bandwidth will be limited by the SQUID bandwidth. For example, the Johnson noise voltage across the junction resistance, so limited, results in an exponentially correlated flux noise [8]. To model such noise sources we will use nonwhite Gaussian noise having mean zero, standard deviation σ and dimensionless, normalized correlation coefficient $R(\tau) = \sigma^{-2} \langle y(t)y(t+\tau) \rangle_t = e^{-|\tau|/\tau_c}$, where τ_c is the noise correlation time. Our results, however, do not rely on the details of the noise correlation since we have focused on frequencies $\omega_0 \ll \tau_c^{-1}$ ($\omega_0 = 1, \tau_c = 0.01$) where the noise is essentially white.

The SQUID output measured is the "shielding flux" $x_s(t) \equiv x(t) - x_e(t)$. We obtain the quasistatic input-output transfer characteristic $g(x_i(t)) = x_s(t)$ by setting $\tau_L \dot{x} = 0$ in the equation of motion and solving for x_s as a function of x_i . In the nonhysteretic regime ($0 \leq \beta < 1$)

a Fourier-Bessel expansion has been obtained for x_s [8,9]:

$$g(x_i) = x_s = \lim_{n'_{\max} \rightarrow \infty} \sum_{n'=1}^{n'_{\max}} M_{n'}(\beta) \sin[2\pi n'(x_i + x_0)];$$

$$M_{n'} \equiv \frac{(-1)^{n'}}{n' \pi} J_{n'}(n' \beta). \quad (1)$$

Figure 1 shows one period of the transfer characteristic, with $x_0 = 1/2$ (modifying x_0 simply translates the curve horizontally). Small ripples visible in the right half of the plot for $\beta = 1$ (solid curve) show the result of truncating (1) after 40 terms. We retained 200 terms when generating the smooth curves in the left half of the plot. The summation approaches the true transfer characteristic more quickly for lower β values. For $\beta = 0.5$ (dashed curve) the truncation error with 40 terms is less than 10^{-10} .

As β is increased from 0 (not shown) to 1, the distance Δx_i from a minimum of the transfer characteristic to the next (higher x_i) maximum *decreases* linearly from 0.5 to 0.18. The minima and maxima heights vary linearly with β and vanish as $\beta \rightarrow 0$.

We will compute the power spectral density via the second moment of the output, $\langle x_s(t)x_s(t + \tau) \rangle_t$. We will then calculate the output SNR and display its maximization for the specific case of the SQUID loop; however, the properties we will discuss are generic to systems with similar transfer characteristics.

We compute the second moment via Rice's method [10,11]. We can apply this technique assuming that the SQUID is always very close to its steady state so that one need only focus on the dynamics of the sinusoidal signal and noise as they are passed through the static nonlinearity given by the transfer characteristic; this implicitly assumes that the signal and noise are both characterized by time constants much larger than the SQUID time constant τ_L , i.e. $\omega_0^{-1}, \tau_c \gg \tau_L$.

Applying Stratonovich's general formula [11] for the second moment of a zero-memory nonlinear transformation of a sine wave plus Gaussian noise, we obtain

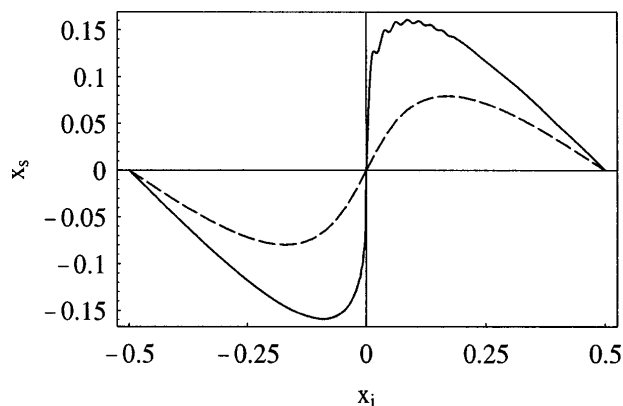


FIG. 1. RF SQUID transfer characteristic $x_s = g(x_i)$ for $\beta = 0.5$ (dashed) and $\beta = 1$ (solid). Right half of plot calculated using $n'_{\max} = 40$, left half using $n'_{\max} = 200$. Bias flux $x_0 = 1/2$.

$$\langle x_s(t)x_s(t + \tau) \rangle_t = \sum_{n=0}^{\infty} \sum_{k=0}^{\infty} \left[\frac{\sigma^n}{2\pi} \int_{-\infty}^{\infty} \int_{-\infty}^{\infty} g(x_i) e^{-ix_i \Omega} dx_i \right. \\ \left. \times J_k(A\Omega) e^{-\sigma^2 \Omega^2 / 2} \Omega^n d\Omega \right]^2 \\ \times \frac{(-1)^{n+k}}{n!} \epsilon_k R^n(\tau) \cos(k\omega_0 \tau), \quad (2)$$

where $\epsilon_{k=0} \equiv 1$, $\epsilon_{k>0} \equiv 2$.

The one-sided power spectral density (in units of Hz^{-1}) follows by using $S(\omega) = 2 \int_{-\infty}^{\infty} \langle x_s(t)x_s(t + \tau) \rangle_t e^{i\omega \tau} d\tau$:

$$S(\omega) = 2 \sum_{n=0}^{\infty} \sum_{k=0}^{\infty} \left[\sum_{n'=1}^{\infty} M_{n'}(\beta) H_{n+k}(2\pi n' x_0) \right. \\ \left. \times J_k(2\pi n' A) (2\pi n' \sigma)^n e^{-2(\pi n' \sigma)^2} \right]^2 \\ \times \frac{\epsilon_k}{n!} G_n(\omega), \quad (3)$$

where

$$H_m(\phi) \equiv \begin{cases} \sin(\phi), & \text{if } m \text{ even,} \\ \cos(\phi), & \text{if } m \text{ odd,} \end{cases} \quad (4)$$

and

$$G_n(\omega) \equiv \begin{cases} \pi \delta(\omega - k\omega_0) & \text{if } n = 0, \\ \frac{n\tau_c}{n^2 + \tau_c^2(\omega - k\omega_0)^2} + \frac{n\tau_c}{n^2 + \tau_c^2(\omega + k\omega_0)^2} & \text{if } n > 0. \end{cases} \quad (5)$$

The spectrum (3) consists of δ functions superimposed on a smooth noise background. Rapid convergence of the summation over k occurs for $k \gg 2\pi n'_{\max} A$. The summation over n will converge quickly if $2\pi n'_{\max} \sigma \ll 1$, with slower convergence if this condition is not met.

We begin by considering the case of bias flux $x_0 = 1/2$. Figure 2 shows a sequence of output SNR gain plots at different input SNR's. In each plot we fix the input SNR R_{in} and vary an input gain parameter γ , setting $A = \gamma$ and $\sigma = \gamma \sqrt{1 + \tau_c^2 \omega_0^2} / \sqrt{8R_{\text{in}} \tau_c}$ [we measure SNR as (signal power at ω_0)/(noise power density at $\omega_0 \times 1 \text{ Hz}$)]. Then we plot output SNR gain $R_{\text{gain}} \equiv R_{\text{out}}/R_{\text{in}}$ vs γ and β (note that $R_{\text{gain}} = R_{\text{out}} - R_{\text{in}}$ if the SNR's are expressed in dB). We have introduced γ to emphasize that we are varying A and σ together, thus keeping the input SNR constant.

The lower left corner of each plot corresponds to the smallest input signal and β , implying nearly linear response and, in all cases, an output SNR virtually identical to the input SNR. The effect of moving out of the lower left corner to higher signal strengths and higher β 's depends on the input SNR.

For high input SNR's, the output SNR rises above the input SNR as we move away from the lower left corner into a region of slightly to moderately nonlinear response. The input signal spends most of its time between approximately $\pm(A + \sigma)$, and the highest output SNR's occur when this deviation fits comfortably within Δx_i , the distance between a minimum of the transfer characteristic and the next maximum. If this deviation exceeds Δx_i , the response becomes highly nonlinear and

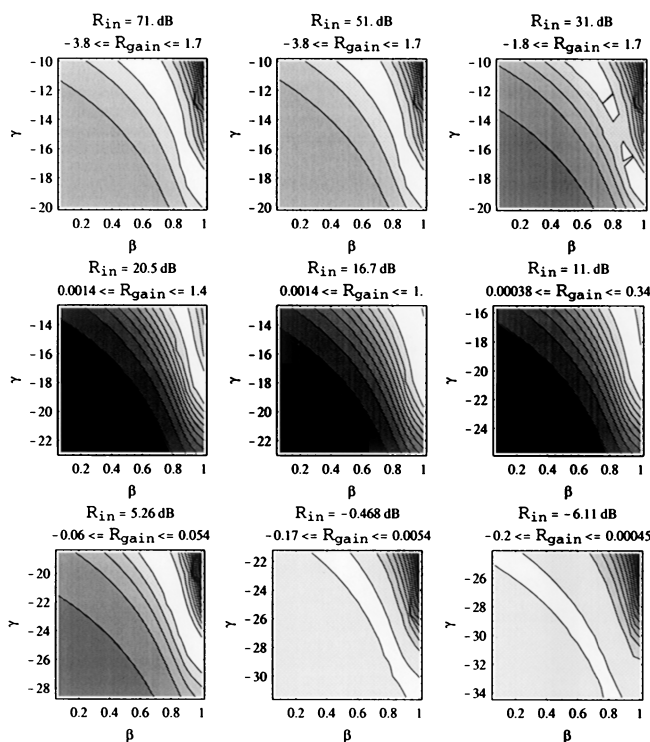


FIG. 2. Output SNR gain R_{gain} (in dB) for various input SNR's, plotted vs input gain γ (in dB) and nonlinearity parameter β . Bias flux $x_0 = 1/2$, $n_{\text{max}}^l = 40$. Grayscale: white is maximum, black is minimum.

the resulting distortion reduces the output SNR below the input SNR. For example, at the top of the $R_{\text{in}} = 71$ dB plot, the input signal spends most of its time between ± 0.1 , and the maximum output SNR occurs for $\beta \approx 0.6$, or $\Delta x_i = 0.31$. As γ is reduced, a larger β and, consequently, smaller Δx_i maximize the output SNR. Note that as the input SNR becomes very large the maximum output SNR gain and loss as well as the shape of the surface appear to converge to fixed values.

In general, any nonadaptive nonlinear filter which has a positive SNR gain for high input SNR's will exhibit a "threshold effect" such that below a specific input SNR threshold the nonlinearity will actually result in an SNR loss. We see this effect in the plots for low input SNR: as we lower the input SNR, the area of highest output SNR approaches the lower left corner where the response is most nearly linear; greater nonlinearity results in the expected SNR loss. (Note that in the two plots with the lowest input SNR we set the highest contour level just below the surface's maximum so that the shape of the nearly-flat "shelf" would be visible—there is very little height difference between the white region and the lightest gray region.)

Note that both the output signal power and noise power (as opposed to their ratio) do decrease rapidly with decreasing β due to the fact that the overall height of the transfer characteristic is proportional to β . Therefore, in any physically realizable system one observes an additional rapid decrease in the measured SNR as $\beta \rightarrow 0$

because the output signal power must compete with the noise floor of the measurement system. Thus, even in the low input SNR case the useful output SNR shows a maximum at some critical $\beta > 0$.

We now turn to the case of arbitrary bias flux. If $x_0 \neq 1/2$, the input signal will not be centered between a transfer characteristic minimum and maximum, and the output SNR may be affected. In fact, the output SNR at the sine wave frequency exhibits a deep trough for input signals centered on one of the extrema of the transfer characteristic. Plotted as a function of x_0 and β , the SNR will exhibit a pattern of spreading troughs as the locations of the transfer characteristic extrema spread with decreasing β . (The SNR surface will be even and periodic in x_0 with period one.)

The dc SQUID [8] consists of a superconducting loop interrupted by two Josephson junctions. Experiments using a high- β dc SQUID generated transfer characteristics qualitatively similar to those discussed above for the rf SQUID. However, it is not necessary to use a set of different dc SQUID's with differing β 's to study a family of transfer characteristics. Instead, the transfer characteristic of the dc SQUID may be modified over a family of curves very similar to those of the rf SQUID by passing various amounts of dc bias current I_b through the Josephson junctions. Recall that β depends on the junction critical current I_c : $\beta \equiv 2\pi LI_c/\Phi_0$. The bias current passed through the junctions can be thought of as effectively changing the junction critical currents. This results in plots analogous to those discussed in the preceding paragraph, but with I_b taking the role of β .

For the rf SQUID, Δx_i decreases linearly with increasing β . For the dc SQUID, experimental data show a linear increase of Δx_i with I_b over the range of Δx_i values possible in the rf SQUID ($0.18 \leq \Delta x_i \leq 0.5$). Inverting these relations, we can use Δx_i as a common scale for comparing rf SQUID results at various β 's with dc SQUID results at various I_b 's. In Fig. 3 we plot the theoretically calculated output SNR obtained from (3) beside a plot of experimental output SNR data from a high- β dc SQUID. The theoretical plot reproduces the experimentally observed pattern of maxima centered at half-integral values of x_0 and surrounded by diverging troughs.

In the experiment, the output noise power fell below the measurement system noise floor for $\Delta x_i > 0.3$. Therefore we added a fixed noise floor to the calculated rf SQUID output noise power as well. Without a noise floor, deep troughs still occur in the theoretical output SNR, but they are narrower. The troughs are therefore *not* due simply to the very small slope near the transfer characteristic extrema reducing the output signal power relative to a fixed noise floor. Rather, nonlinear response is modifying the output signal and noise powers by different amounts.

The comblike pattern noticeable along the left edge of the theoretical plot (corresponding to β 's near 1.0) results from small oscillations near the transfer characteristic

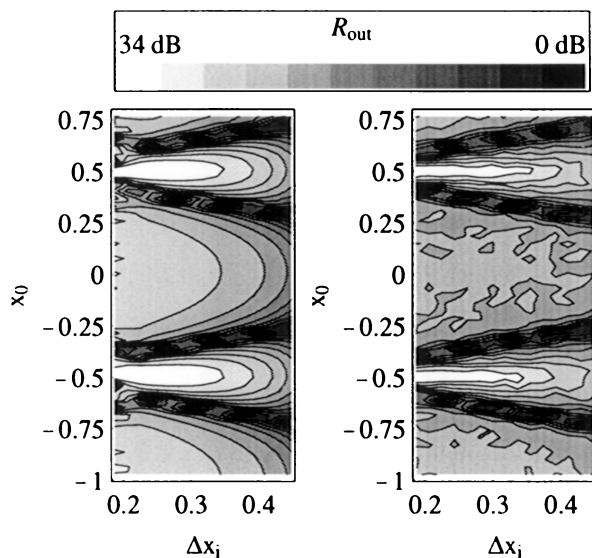


FIG. 3. Theoretical (left) and experimental (right) output SNR as a function of x_0 and Δx_i , with $\gamma = 0.001$, $R_{in} = 34$ db, and $n'_{max} = 40$.

extrema caused by truncating the Bessel function summation at $n' = 40$ (see Fig. 1).

As we have mentioned, for the rf SQUID the largest possible Δx_i is 0.5 (obtained as $\beta \rightarrow 0$). What happens in the dc SQUID if we raise I_b beyond the value which gives $\Delta x_i = 0.5$? Interestingly, the transfer characteristic actually changes shape and develops a new, flat region centered between each minimum and the next maximum. This is qualitatively different from an rf SQUID transfer characteristic. However, such transfer characteristics may be approximated by, e.g., a piecewise linear function, and an analytical result for the SNR may still be obtained.

To summarize, an important observation of this Letter is the β -dependent SNR optimization; recall that β is a design parameter that is *independent* of the input SNR. As we cross above the $\beta = 1$ threshold, we encounter the hysteretic regime. Here the usual SR behavior has been well documented [2]; however, there is no longer an optimization with respect to β .

In related work [5] a “stochastic resonance without tuning” scenario in a model of a neural network subject to a wideband signal in white noise was considered, with a typical element characterized by its (sigmoidal) firing rate vs signal amplitude characteristic. The “resonance” in the Fourier transform of the input-output cross-correlation function was found to correspond to a critical slope of the transfer characteristic. The authors characterized regimes wherein the noise-induced firing could benefit from this “noise-induced linearization” as well as from SR.

For the class of (nonhysteretic) systems described here, our results demonstrate a particularly efficient means of optimizing the output SNR. Our work shows that the effects depicted in Figs. 2 and 3 may be generic to nonlinear, nonhysteretic dynamic systems that respond via transfer characteristics of the type shown in Fig. 1;

such characteristics are typical products of experiments on nonlinear devices. No assumptions regarding the existence of a threshold or an *a priori* form for a crossing rate have been made. For the hysteretic case, the nonlinearity parameter controls the separation of the stable states as well as the height of the “energy barrier” separating them. In this hysteretic case, the SR literature documents that the lower the barrier height, the higher the SNR of the response to a fixed input sine wave plus noise. Below the hysteresis threshold ($\beta = 1$ for the rf SQUID) we obtain the above-described maximum in the SNR at a critical value of the nonlinearity parameter β .

A. R. B acknowledges support from the Office of Naval Research through Grant No. N0001496AF00002 as well as the Internal Research program at SPAWARSYSCEN SD, and NATO-CRG 131464. MEI was supported in part by a grant from the DoD high performance computing initiative in Computational Electronics and Nanoelectronics. We gratefully acknowledge fruitful conversations with L. Gammaitoni.

*Electronic address: inchiosa@nosc.mil

†Electronic address: bulsara@nosc.mil

‡Electronic address: andy.hibbs@qm.com

§Electronic address: brian.whitecotton@qm.com

- [1] For good overviews, see K. Wiesenfeld and F. Moss, *Nature (London)* **373**, 33 (1995); A. Bulsara and L. Gammaitoni, *Phys. Today* **49**, No. 3, 39 (1996); L. Gammaitoni, P. Hanggi, P. Jung, and F. Marchesoni, *Rev. Mod. Phys.* **70**, 1 (1998).
- [2] A. Hibbs, A. Singsaas, E. Jacobs, A. Bulsara, J. Bekkedahl, and F. Moss, *J. Appl. Phys.* **77**, 2582 (1995); R. Rouse, S. Han, and J. Lukens, *Appl. Phys. Lett.* **66**, 108 (1995); A. Bulsara, M. Inchiosa, and L. Gammaitoni, *Phys. Rev. Lett.* **77**, 2162 (1996); M. Inchiosa, A. Bulsara, and L. Gammaitoni, *Phys. Rev. E* **55**, 4049 (1997).
- [3] M. Dykman, D. Luchinsky, R. Mannella, P. V. E. McClintock, N. Stein, and N. Stocks, *J. Stat. Phys.* **70**, 479 (1993).
- [4] J. Collins, C. Chow, and T. Imhof, *Phys. Rev. E* **52**, R3321 (1995); *Nature (London)* **376**, 236 (1995); A. Bulsara and A. Zador, *Phys. Rev. E* **54**, R2185 (1996); C. Heneghan, J. Collins, C. Chow, T. Imhoff, S. Lowen, and M. Teich, *Phys. Rev. E* **54**, R2228 (1996); M. Stemmler, *Network* **7**, 687 (1996); F. Chapeau-Blondeau, *Phys. Rev. E* **55**, 2016 (1997).
- [5] D. Chialvo, A. Longtin, and J. Muller-Gerking, *Phys. Rev. E* **55**, 1798 (1997).
- [6] S. Bezuikhov and I. Vodyanoy, *Nature (London)* **385**, 319 (1997).
- [7] F. Chapeau-Blondeau and X. Godiver, *Phys. Rev. E* **55**, 1478 (1997).
- [8] A. Barone and G. Paterno, *Physics and Applications of the Josephson Effect* (Wiley, New York, 1982).
- [9] S. Erne, H. Hahlbohm, and H. Lubbig, *J. Appl. Phys.* **47**, 5440 (1976).
- [10] S. Rice, in *Selected Papers on Noise and Stochastic Processes*, edited by N. Wax (Dover, New York, 1954).
- [11] R. Stratonovich, *Topics in the Theory of Random Noise* (Gordon and Breach, New York, 1963), Vol. 1.